

UC Irvine

UC Irvine Previously Published Works

Title

Plasmoid propagation in a transverse magnetic field and in a magnetized plasma

Permalink

<https://escholarship.org/uc/item/6qr590fj>

Journal

Physics of Fluids, 31(12)

ISSN

00319171

Authors

Wessel, F. J
Hong, R.
Song, J.
[et al.](#)

Publication Date

1988

DOI

10.1063/1.866897

Peer reviewed

Plasmoid propagation in a transverse magnetic field and in a magnetized plasma

F. J. Wessel, R. Hong,^{a)} J. Song, A. Fisher, N. Rostoker, A. Ron,^{b)} R. Li,^{a)} and R. Y. Fan^{c)}

Department of Physics, University of California, Irvine, California 92717

(Received 8 April 1988; accepted 19 August 1988)

The propagation of plasmoids (neutralized ion beams) in a vacuum transverse magnetic field has been studied in the University of California, Irvine laboratory for several years [Phys. Fluids **24**, 739 (1981); **25**, 730, 2353 (1982); **26**, 2276 (1983); J. Appl. Phys. **64**, 73 (1988)]. These experiments have confirmed that the plasmoid propagates by the $\mathbf{E} \times \mathbf{B}$ drift in a low beta and high beta plasmoid beam ($0.01 < \beta < 300$), where β is the ratio of beam kinetic energy to magnetic field energy. The polarization electric field \mathbf{E} arises from the opposite deflection of the plasmoid ions and electrons, because of the Lorentz force, and allows the plasmoid to propagate undeflected at essentially the initial plasmoid velocity. In these experiments, plasmoids (150 keV, 5 kA, 50–100 A/cm², 1 μ sec) were injected into transverse fields of $B_t = 0$ –400 G. Anomalous fast penetration of the transverse magnetic field has been observed as in the “Porcupine” experiments [J. Geophys. Res. **91**, 10,183 (1987)]. The most recent experiments are aimed at studying the plasmoid propagation dynamics and losses in the presence of a background, magnetized plasma which is intended to short the induced polarization electric field and stop the beam. Background plasma was generated by TiH₄ plasma guns fired along B_t to produce a plasma density, $n_p = 10^{12} - 10^{14}$ cm⁻³. Preliminary results indicate that the beam propagation losses increase with the background plasma density; compared to vacuum propagation, roughly a 50% reduction in ion current density was noted 70 cm downstream from the anode for $n_p \sim 10^{13}$ cm⁻³. Principal diagnostics include magnetically insulated Faraday cups, floating potential probes, calorimeters, microwave interferometer, and thermal-witness paper.

I. INTRODUCTION

The first paper on plasmoid motion across a transverse magnetic field was published in 1931.¹ The subject is fundamental to plasma physics and has applications to geomagnetic storms and solar wind penetration into the geomagnetic field,² injection of a plasmoid into a magnetic containment device,³ and the dynamics of pinches.⁴ The present work is concerned with the propagation of a neutralized ion beam (plasmoid) in and above the ionosphere in a background magnetic field and a low density partially ionized plasma. The neutralized ion beam may be generated directly as in our experiments, or it may begin as a beam of neutral atoms that is ionized by background gas and plasma at low altitude.

We define $\beta = 4\pi nMV^2/B^2$ as the ratio of the beam kinetic energy density to the magnetic field energy density. Here V is the beam velocity, M is the ion mass, n is the beam ion density, and B is the background magnetic field. Only the case $\beta \gg 1$ is considered. Three phases of propagation are illustrated in Fig. 1. The idealization of the diamagnetic phase to a perfect conductor suggests that the exclusion of the field should result in simple ballistic propagation. After

the magnetic field has penetrated the beam, propagation would be expected by means of self-polarization and $\mathbf{E} \times \mathbf{B}$ drift as observed for low beta beams.^{5,6}

A series of rocket experiments⁷ launched the “Porcupine plasma jet.” Nearly undeflected propagation of the dense ($n_{\text{beam}} \gg n_{\text{plasma}}$) and fast heavy ion beam ($V \approx 1.7 \times 10^4$ m/sec; $M = 131m_p$) was observed in the magnetized ionospheric plasma. The beam passed from phase I to phase III of Fig. 1 in a time much shorter than that expected from classical diffusion. Propagation was dominated by phase III. This was attributed to anomalous diffusion caused by an instability driven by the diamagnetic current.

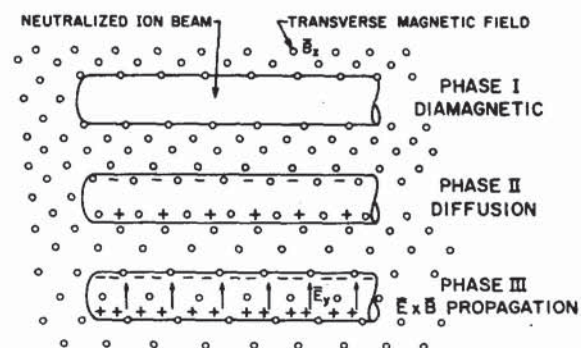


FIG. 1. Here we see three phases of propagation of a high beta neutralized ion beam.

^{a)} Permanent address: Institute of Atomic Energy, P.O. Box 275, Beijing, People's Republic of China.

^{b)} Permanent address: Physics Department, Technion, Haifa, Israel.

^{c)} Permanent address: Changsha Institute of Technology, Changsha, Hunan, People's Republic of China.

On the other hand, in recent computer⁸ simulation studies of this problem, the diamagnetic phase was dominant and the background plasma and magnetic field were diverted around the beam. We seek to understand these apparently contradictory conclusions by doing laboratory experiments where much more detailed measurements are possible, and analytic theory and computer simulations are guided by the experimental results.

II. CROSS-FIELD PROPAGATION IN VACUUM

A. Description of experiment

The experiment is illustrated in Fig. 2. The Marx generator consists of six stages of 50 kV, 0.7 μF capacitors and delivers an output voltage in the range 100–200 kV. The Marx output is connected to a magnetically insulated ion diode as illustrated in Fig. 3. It is an annular diode with an anode–cathode spacing of 13 mm. The magnetic insulation field is 2–2.5 kG with a field rise time of 40 μsec . At 150 kV output voltage the diode produces a 4 kA beam of ions—50 A/cm² and 1 μsec duration with a peak ion energy in the range of 100–120 keV; this value of ion energy was measured by time of flight and is lower than the output voltage resulting from inductive voltage division in the output transmission line. Ions are produced by surface flashover of a 0.8 mm polyethylene sheet with stainless steel pins mounted on the anode electrode. The approximate ion composition in the beam is 75% H⁺, 15% C⁺, 10% CH_n⁺.⁹

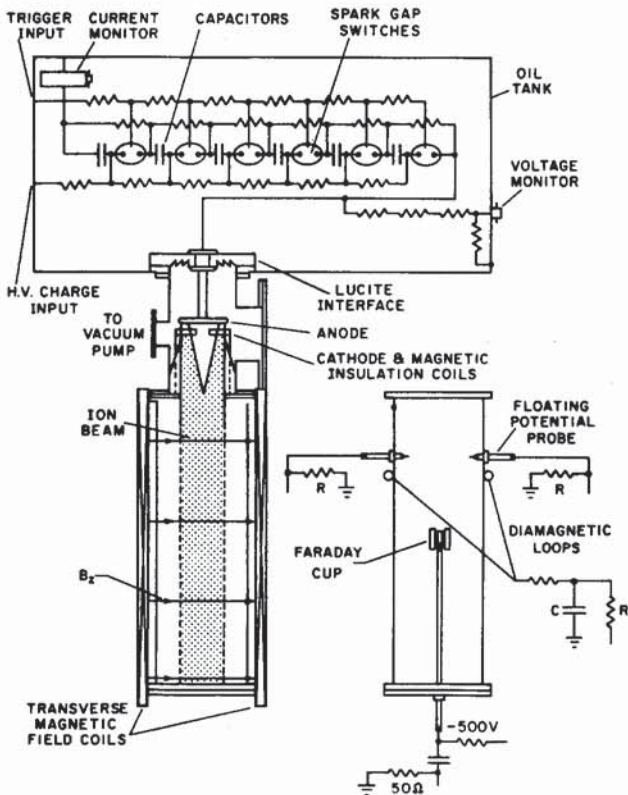


FIG. 2. Schematic diagram of experimental apparatus for the study of ion beam propagation. The drift tube illustration on the lower right-hand side displays the location of various diagnostics.

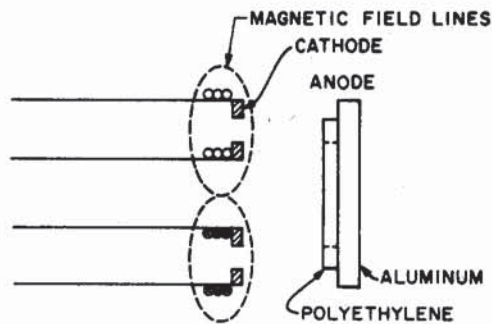


FIG. 3. Magnetically insulated ion diode.

Two pairs of field coils were used to generate B_z with dimensions: 2.3 m \times 0.5 m with five turns and 1.15 m \times 0.5 m with five turns. Each pair of coils had a spacing of 0.4 m and was driven by a 3 kV, 4 \times 580 μF capacitor bank. The field strengths were 121 G/kV for the longer coil and 190 G/kV for the shorter coil with rise time of 0.7 msec. Lucite drift tubes were used to study the beam propagation over the 2 m transverse field region. The tube diameters were nominally 26 cm and were installed in 0.5 m length sections or a single 2 m length section. Vacuum was 10^{-5} Torr.

Several diagnostics were used in the experiments. The ion current density was measured using biased Faraday cups (–500 V bias) with small magnets to suppress secondary electron emission. A \dot{B} loop with a 12 msec integration time was used to measure the B_z field. The diamagnetic signal induced by the beam as it entered the field was measured by a pair of fast \dot{B} loops with a 11.2 μsec integration time constant to prevent the slower B_z field from being recorded. These diamagnetic loops have a diameter of 27 mm, 20 turns each, with a sensitivity of 0.2 V/G. Both probes were wrapped in conductive cloth to shield the electrical noise. One coil was located in vacuum 45 cm downstream from the anode coaxial with the ion beam and the drift tube. The other coil was located outside the beam. A pair of floating potential Langmuir probes was used to measure the polarization electric field E_y .¹⁰ These probes were made of rigid coaxial cables with the center conductor exposed about 5 cm and inserted into the drift tube through Wilson seals. This allowed measurement of the potential difference $\Delta\Phi$ over a known probe separation distance. Signals from these probes were sent to a differential amplifier and recorded. The existence of E_y was verified by several tests: $\Delta\Phi$ changes sign if the sign of B_z is changed, $\Delta\Phi = 0$ if the probes' tips are touching and linearly increases with probe tip separation, and $\Delta\Phi = 0$ if $B_z = 0$. Thermal graphic paper was used as a witness plate to trace the beam location and radial profile and to estimate the beam divergence and beam energy. The paper shows a distinct and noticeable color change in the range of 1–5 J/cm², beyond which no additional color change occurs.

B. Experimental results

Net current measurements with a Rogowski loop and floating probe measurements verified that the ion beam in

the drift tube was charge and current neutralized. Damage patterns on thermal paper located 40 cm and 70 cm downstream showed that the beam divergence was $3^\circ\text{--}4^\circ$ when the diode voltage was above 100 kV. Some experimental parameters are given in Table I, where ρ_i is the ion gyroradius based on the beam velocity V_0 and $\epsilon = 4\pi nMc^2/B^2$ is the dielectric constant.

Beam propagation across the transverse magnetic field was evaluated with Faraday cups. Figure 4 shows results. Although the angular spread of the beam leads to a significant decrease of current density with propagation distance, there is very little decrease in current density as the magnetic field is changed over a few orders of magnitude and β changed from 0.01 to 300. The magnetic field B_z does not significantly change beam propagation.

Diamagnetic signals ΔB_0 were measured at 50 cm downstream from the diode and are shown in Fig. 5. The value of beta was changed by holding the diode voltage fixed at 150 kV and changing the magnetic field B_z . Here ΔB_m is the largest change in magnetic field just outside the beam at $r \approx 10$ cm. The magnetic field change was also measured by a similar \vec{B} probe on the beam axis. The polarity of ΔB_i was opposite to ΔB_0 indicating that the field decreases inside the beam and increases outside. We see that $\Delta B_0/B_z \ll 1$ and $\Delta B_i/B_z \ll 1$; both signals increase with increasing beta but the above inequalities are preserved for beta up to a value of 400. These facts confirm that the magnetic field penetrates the plasma in a time that is small compared to the current rise time which is about $0.5 \mu\text{sec}$, so that only a slight perturbation of the magnetic field is ever observed, although the beam is a good conductor.

Measurements of the polarization electric field E_y , 40 cm downstream from the anode, are displayed in Fig. 6 for fixed V_d and varying values of B_z ; the probe tip separation was 2 cm. These data show that the peak value of E_y (displayed in bold type for convenience) increases linearly with B_z and is comparable to the theoretical value computed from $E_y = V_0 B_z / c$ over the range of parameters studied. This is consistent with the fast penetration of the magnetic field and propagation by means of the $\mathbf{E} \times \mathbf{B}$ drift.

III. CLASSICAL AND ANOMALOUS DIFFUSION

Consider the idealization of a perfectly conducting cylinder in a transverse magnetic field as illustrated in Fig. 7. The magnetic field is given by $\mathbf{B} = \nabla\Psi$, where $\nabla^2\Psi = 0$ subject to the boundary conditions

$$\lim_{r \rightarrow \infty} \Psi = B_0 r \cos \theta, \quad (1)$$

TABLE I. Relevant experimental parameters. $L = 50\text{--}200$ cm, $r = 10$ cm, $v_0 = 4.4 \times 10^8$ cm/sec (for 100 keV beam), $n_i = 1.42 \times 10^{11}$ cm $^{-3}$ (for $J = 10$ A/cm 2).

| B_z (G) | 50 | 89 | 149 | 194 | 239 | 284 | 328 | 373 |
|--------------------------|-----|------|------|------|------|------|------|------|
| ρ_i (cm) | 920 | 516 | 308 | 237 | 192 | 161 | 140 | 123 |
| $\epsilon (\times 10^4)$ | 107 | 33.7 | 12.0 | 7.10 | 4.67 | 3.30 | 2.48 | 1.92 |

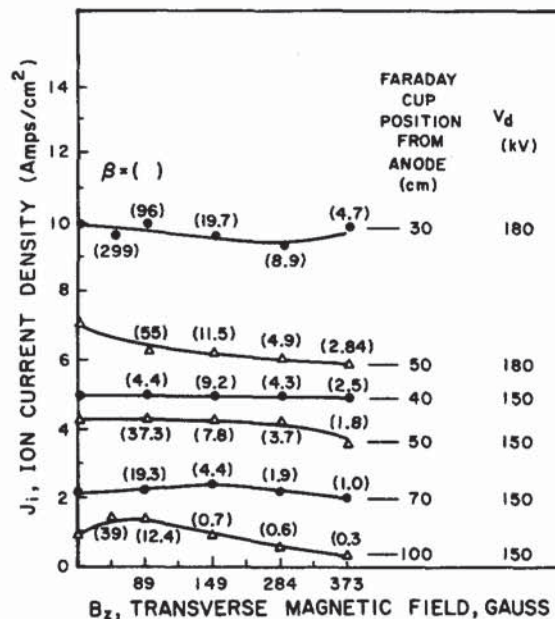


FIG. 4. Beam propagation across the transverse magnetic field with the annular diode. The values of beta are indicated in parentheses.

$$\frac{\partial \Psi}{\partial r} = 0, \quad \text{for } r = a. \quad (2)$$

The solution is $\Psi = B_0 [r + (a^2/r)] \cos \theta$. If $\theta = -\pi/2$,

$$B_\theta = B_z = B_0 [1 + (a^2/r)]. \quad (3)$$

At the surface of the beam $B_z = 2B_0$ and at $r = 2a$, $B_z = 1.25 B_0$. In Table II we compare values of the calculated

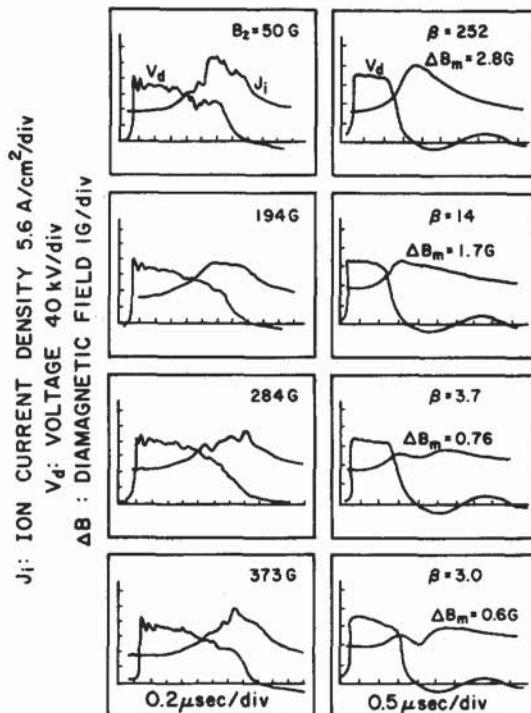


FIG. 5. Measurements of diode voltage, current density, and diamagnetic field at 50 cm from the anode; β is changed by changing the magnetic field.

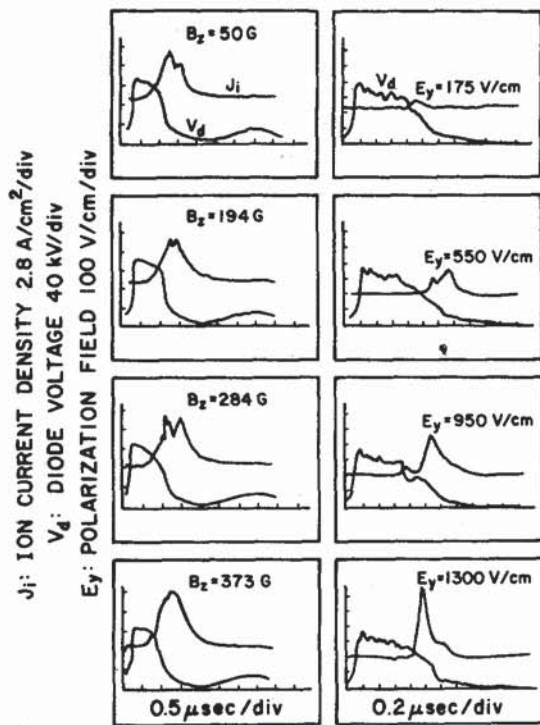


FIG. 6. Measurements of diode voltage, current density, and polarization electric field at 40 cm from the anode for the annular diode.

diamagnetic signal for a perfect conductor, $\Delta B = B_0$, just outside the beam with the experimentally measured diamagnetic signal ΔB_m .

For a perfect conductor as in Fig. 7 the current should be localized on the surface, i.e.,

$$J_x = J_x(a, \theta) \delta(r - a), \quad (4)$$

where

$$J_x = (c/4\pi) B_\theta = - (c/2\pi) B_0 \sin \theta. \quad (5)$$

For a finite classical conductivity magnetic diffusion should take place on a time scale given by

$$(\Delta r)^2 = D \Delta t, \quad (6)$$

where

$$D = (c/\omega_p)^2 (1/\tau_{ei}), \quad (7)$$

$\omega_p^2 = 4\pi n e^2/m$, n is the electron density, Δr is the depth of penetration of the magnetic field or the current density after time Δt , $\tau_{ei} = 3 \times 10^4 (T^{3/2}/n)$ sec is the electron-ion collision

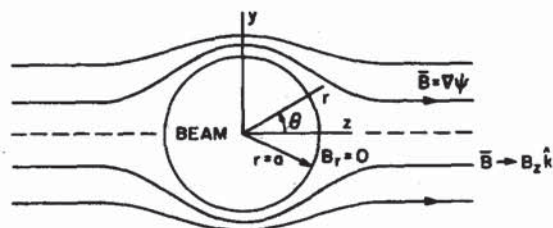


FIG. 7. Diamagnetism of a perfectly conducting cylindrical beam.

TABLE II. Comparison of experimentally measured external diamagnetic signal (ΔB_m) with the expected value (B_0) for a perfect conductor.

| B_0 G | 50 | 89 | 149 | 194 | 239 | 284 | 328 |
|------------------------|-----|------|------|------|------|------|-----|
| ΔB_m G | 2.8 | 2.7 | 2.2 | 1.7 | 1.7 | 0.8 | 0.7 |
| $100 \Delta B_m / B_0$ | 5.6 | 3.04 | 1.48 | 0.88 | 0.72 | 0.28 | 0.2 |
| β | 252 | 45 | 37 | 14 | 11.4 | 3.7 | 3.3 |

time, and T is the electron temperature in electron volts. (For a vacuum of 10^{-5} Torr, only Coulomb collisions need be considered.) The electron temperature has not been measured. If we assume $T = 10$ eV, $\Delta r = 10$ cm, and $n = 3 \times 10^{11} \text{ cm}^{-3}$, then $c/\omega_p = 1$ cm, $\tau_{ei} = 10^{-6}$ sec, and $\Delta t \approx 100 \mu\text{sec}$. The observed time is much less than $1 \mu\text{sec}$ and we conclude that the diffusion time is certainly much less than this classical estimate.

A similar conclusion was reached in the analysis of data from the "Porcupine" experiments.⁷ (This conclusion is distinct from the computer simulations of Mankofsky *et al.*⁸) Mishin *et al.* have explained⁷ the fast diffusion as an anomalous process attributed to a transverse electron drift current-driven electrostatic instability excited by the diamagnetic current. Initially this current is concentrated near the surface of the beam and linear instability criteria are easily satisfied. After some diffusion has taken place, the current density becomes too small for most instabilities. In any case, a satisfactory theory must explain the difference between the fast diffusion for a plasmoid and the slow diffusion for pinches. If the diffusion rate were as fast for pinches, the phenomena would not be observed and the current densities in pinches are usually much larger than for the present plasmoid experiments.

For further consideration we simplify the geometry and consider a one-dimensional problem as illustrated in Fig. 8. The magnetic field is assumed to be $\mathbf{B} = (0, 0, B_z)$, where $B_z = B_z(x, t)$, and at $t = 0$,

$$B_z = \begin{cases} B_0, & x < 0, \\ 0, & x > 0. \end{cases}$$

Maxwell's equations for the problem are

$$\frac{\partial E_y}{\partial x} = \frac{1}{c} \frac{\partial B_z}{\partial t}, \quad (8)$$

$$-\frac{\partial B_z}{\partial x} = \frac{4\pi}{c} j_y + \frac{1}{c} \frac{\partial E_y}{\partial t}. \quad (9)$$

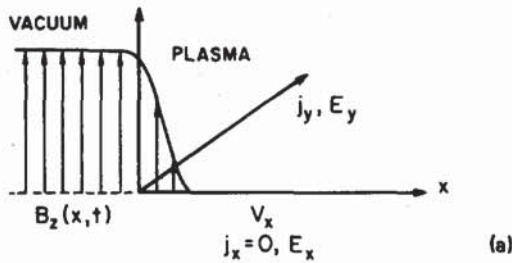
If there exists a relation of the form $j_y = \sigma E_y$ and $4\pi\sigma \gg |(\partial E_y / \partial t) / E_y|$, then Eqs. (8) and (9) combine to give a diffusion equation

$$\frac{\partial}{\partial x} D \frac{\partial B_z}{\partial x} = \frac{\partial B_z}{\partial t}, \quad (10)$$

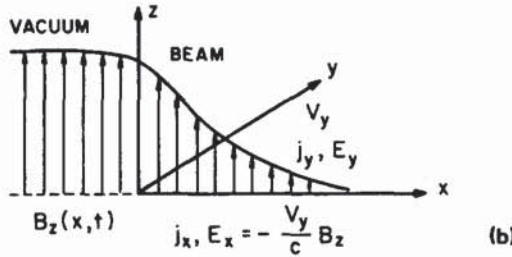
where

$$D = c^2 / 4\pi\sigma. \quad (11)$$

To determine σ , we consider the generalized form of Ohm's law¹¹:



DIFFUSION OF MAGNETIC FIELD INTO A Z PINCH OR \odot PINCH. (LONGITUDINAL POLARIZATION)



DIFFUSION OF MAGNETIC FIELD INTO A PROPAGATING NEUTRALIZED ION BEAM. (TRANSVERSE POLARIZATION)

FIG. 8. Boundary conditions illustrating polarization transverse and longitudinal to plasma motion.

$$\left(\frac{m}{ne^2}\right)\left(\frac{\partial \mathbf{j}}{\partial t}\right) + \frac{\mathbf{j}}{\sigma_0} + \frac{(\mathbf{j} \times \mathbf{B})}{nec} = \mathbf{E} + \frac{\mathbf{V} \times \mathbf{B}}{c} + \frac{\nabla P_e}{n_e}, \quad (12)$$

$\sigma_0 = (ne^2/m)\tau_e$, \mathbf{V} is the plasmoid velocity viewed from the laboratory frame, P_e is the electron pressure, and $\Omega_e = eB_z/mc$ is the electron cyclotron frequency. The last term $\nabla P_e/n_e$ can be neglected. Also, τ_e is the collision frequency which we assume is τ_{ei} from classical Coulomb collisions. [According to Mishin *et al.*⁷ it is $\tau_e = (\Omega_e \Omega_i)^{-1/2}$ because of turbulence; in any case $\Omega_e \tau_e \gg 1$.] The appropriate form for the generalized Ohms law is

$$\frac{\partial j_x}{\partial t} + \frac{j_x}{\tau_e} - \Omega_e j_y = E'_x \left(\frac{\sigma_0}{\tau_e}\right), \quad (13)$$

$$\frac{\partial j_y}{\partial t} + \frac{j_y}{\tau_e} + \Omega_e j_x = E'_y \left(\frac{\sigma_0}{\tau_e}\right), \quad (14)$$

where $E'_x = E_x + (1/c)V_y B_z$ and $E'_y = E_y - (V_x/c)B_z$ are the electric fields in the moving frame. If E'_x, E'_y, Ω_e change little during a cyclotron period, the solution averaged over a cyclotron period is

$$j_x = \sigma_0(E'_x - \Omega_e \tau_e E'_y) / [1 + (\Omega_e \tau_e)^2], \quad (15)$$

$$j_y = \sigma_0(\Omega_e \tau_e E'_x + E'_y) / [1 + (\Omega_e \tau_e)^2]. \quad (16)$$

The problem illustrated in Fig. 8(a) corresponds to a pinch. Since electrons and ions move together in the x direction $j_x = 0$, $V_x \neq 0$, and $V_y = 0$; from Eqs. (15) and (16), $E_x = \Omega_e \tau_e j_y / \sigma_0$ and

$$j_y = \sigma_0 E'_y = \sigma_0 [E_y - (V_x/c)B_z]. \quad (17)$$

Diffusion in the moving frame is determined by the diffusion coefficient $D = c^2/4\pi\sigma_0$. Unless the collision time τ_e is determined by turbulence, the diffusion would be very slow; turbulence might be expected in the initial stages when the current density is very high, but after a short time the current density would drop and collision time τ_e should be classical. This agrees with the observed behavior of pinches.¹²

The problem illustrated in Fig. 8(b) corresponds to plasmoid or beam propagation. In order to propagate the beam must polarize in the x direction so that $E'_x = E_x + (V_y B_z/c) = 0$ and $V_x = 0$. Equations (15) and (16) then reduce to

$$j_y = \sigma_0 E_y / [1 + (\Omega_e \tau_e)^2], \quad j_x = -(\Omega_e \tau_e) j_y. \quad (18)$$

The conductivity $\sigma = \sigma_0 / [1 + (\Omega_e \tau_e)^2]$ is greatly reduced compared to σ_0 because $\Omega_e \tau_e \gg 1$. The diffusion equation (10) becomes nonlinear with

$$D = (c^2/4\pi\sigma_0) [1 + (\Omega_e \tau_e)^2]. \quad (19)$$

An estimate of the penetration time is that it is reduced by the factor $(\Omega_e \tau_e)^2$ compared to the previous estimate of 100 μsec based on Eqs. (6) and (7). For the same assumed data and $B_0 = 100$ G,

$$(\Omega_e \tau_e)^2 \cong 3 \times 10^6$$

and

$$\Delta t = (\Delta r \omega_p / c)^2 [\tau_e / (\Omega_e \tau_e)^2] \cong 0.3 \text{ nsec}. \quad (20)$$

If we assume with Mishin *et al.*⁷ that $\tau_e \sim (\Omega_e \Omega_i)^{-1/2} \sim 23.5$ nsec, then $(\Omega_e \tau_e)^2 \cong M/m = 1.8 \times 10^3$ and $\Delta t \cong 1.3$ nsec. It is somewhat of a curiosity that decreasing the collision time increases the diffusion time. The difference between a pinch and a plasmoid propagating across a magnetic field is the factor $(\Omega_e \tau_e)^2$. We see that $(\Omega_e \tau_e)^2 \gg 1$ whether or not the plasma is turbulent. We have thus accounted for the short penetration time and the very small diamagnetic signal. The present experimental data is insufficient to come to a conclusion about turbulence.

The nonlinear diffusion equation with D given by Eq. (19) has previously been studied by Felber *et al.* in connection with a plasma switch application.¹³ Detailed solutions are given for the problem in plane geometry. In this paper ion conductivity is also included so that

$$\sigma = ne^2 \{ (\tau_e / m) / [1 + (\Omega_e \tau_e)^2] + (\tau_i / M) / [1 + (\Omega_i \tau_i)^2] \}. \quad (21)$$

If $\Omega_e \tau_e > (M/m)^{1/2}$ the ion conductivity becomes dominant. The calculation of Eq. (20) should accordingly be multiplied by the factor $(M/m)^{3/2}$ to give a classical estimate of $\Delta t \cong 0.2 \mu\text{sec}$.

Computer simulation studies of this problem have been carried out by Tajima and his collaborators.¹⁴ For $a_i/L \sim 100$, the magnetic field penetration is anomalously fast and for $a_i/L < 10$ the penetration is much slower. The computer model involves slab geometry; L is the slab thickness and $a_i = V_0/\Omega_i$ is the ion gyroradius. In the experiments $a_i/r \gg 1$ in all cases observed; the penetration time was too short

to observe in all cases when a_i/r was varied over a factor of 5. In earlier unpublished results obtained at the University of California at Irvine, there is some evidence for slower penetration when the plasmoid is produced by a plasma gun where $a_i/r < 1$.

IV. CROSS-FIELD PROPAGATION IN PLASMA

To produce the background plasma we used 15 small circular plasma guns connected in parallel. Each one has an annular gap filled with TiH_4 . The density of the plasma produced by the plasma gun was measured by a 60 GHz microwave interferometer. The plasma density in the drift tube increased approximately linearly with increasing plasma gun voltage V_{PG} . When $V_{\text{PG}} = 4$ kV, the average plasma density was about $10^{13}/\text{cm}^3$.

The electric polarization was measured¹⁵ for various magnetic fields and values of V_{PG} (plasma density). The results are shown in Fig. 9. It is apparent that the plasma reduces the polarization electric field and it becomes negligible at about 10^{13} cm^3 . For a density of the order of the beam density or less, there is little effect.

The beam deflection was also measured with red cellulose witness plates. When $V_{\text{PG}} = 3\text{--}4$ kV, the beam deflection agrees quite well with a simple calculation based on the Lorentz force, which is consistent with the vanishing of the polarization electric field. For plasma density less than the beam density, or no plasma density, no deflection was observed.¹⁵

In-beam diamagnetic measurements showed fast penetration on a time scale much less than $1 \mu\text{sec}$ with or without a background plasma. If we consider Eqs. (15) and (16), the appropriate conditions with a dense background plasma are $V_x = 0$ and $E_x = 0$ instead of $E_x + (V_y B_z / c) = 0$. Therefore

$$J_y \approx \sigma_0 E_y / [1 + (\Omega_e \tau_e)^2] + n_e V_y. \quad (22)$$

This leads to a modified diffusion equation

$$\frac{\partial}{\partial x} D \frac{\partial B_z}{\partial x} + 2V_y (\Omega_e \tau_e) \frac{\partial B_z}{\partial x} = \frac{\partial B_z}{\partial t}, \quad (23)$$

with D given by Eq. (19). The first term dominates if

$$\left| \frac{1}{B_z} \frac{\partial B_z}{\partial x} \right| > 2 \frac{V_y}{\Omega_e} \left(\frac{\omega_p}{c} \right)^2. \quad (24)$$

The solution of the nonlinear equation is more like a wave¹³ and Eq. (24) would be satisfied at the front of the "magneto-resistive" wave so that Eq. (23) should produce fast diffusion similar to Eq. (10).

V. CONCLUSIONS

It has been established that a high beta plasmoid propagates across a transverse magnetic field without significant deflection. The mechanism is not diamagnetic flux exclusion and ballistic propagation as first anticipated, but it is instead electric polarization of the plasmoid and $\mathbf{E} \times \mathbf{B}$ drift as in a low beta plasmoid. The magnetic field penetrates the plasmoid so rapidly that no significant diamagnetic effect can be observed. Essentially, the unperturbed magnetic field is present inside the plasmoid at all observable times. This behavior of a plasmoid is completely different from the behavior of a metallic conducting projectile. It is also completely different from a Z or \odot pinch. Indeed, if the field slipped across the particles as fast in a pinch, a pinch would never be observed. We have explained the difference physically by the fact that the polarization for the pinch is longitudinal (electric field parallel to the motion) and transverse for the propagating plasmoid. The question of turbulence as proposed to explain the "Porcupine experiments" has not been resolved. Although there may be turbulence it is not essential to explain the fast penetration of the magnetic field.

With $\mathbf{E} \times \mathbf{B}$ propagation, the electric field near the plasmoid surface must be different than in the interior.⁵ Therefore the surface must erode and this is the mechanism of beam loss that has been observed in computer simulations, but not yet in the laboratory. In the laboratory, losses have been observed by expansion of the beam from angular divergence in a small radius drift tube. A new system has been developed that involves a much smaller angular divergence of the plasmoid and a larger drift tube to study the erosion losses.

ACKNOWLEDGMENTS

The authors are especially grateful to T. Tajima and B. S. Newberger at the Institute for Fusion Studies for informative and stimulating discussions.

This research was supported by AFOSR/SDI.

¹S. Chapman and V. C. A. Ferraro, *J. Geophys. Res.* **36**, 77 (1931).

²V. C. A. Ferraro, *J. Geophys. Res.* **57**, 15 (1952).

³D. A. Baker and J. E. Hammel, *Phys. Fluids* **8**, 713 (1965); W. M. Bos-

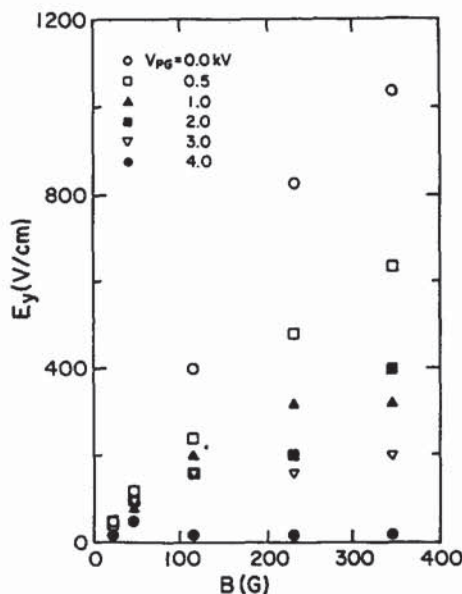


FIG. 9. Polarization electric field versus transverse magnetic field at various plasma gun voltage.

- tick, Phys. Rev. **104**, 292 (1956); J. L. Tuck, Phys. Rev. Lett. **3**, 313 (1959).
- ⁴M. N. Rosenbluth, in *Plasma Physics and Thermonuclear Research*, edited by C. L. Longmire, J. L. Tuck, and W. B. Thompson (Pergamon, London, 1963), Vol. II, p. 271; H. Dickinson, W. H. Bostick, J. N. DiMarco, and S. Koslov, Phys. Fluids **5**, 1048 (1962).
- ⁵W. Peter and N. Rostoker, Phys. Fluids **25**, 730 (1982).
- ⁶H. Ishizuka and S. Robertson, Phys. Fluids **25**, 2353 (1982).
- ⁷E. V. Mishin, R. A. Treumann, and V. Y. Kapitanov, J. Geophys. Res. **91**, 10,183 (1986).
- ⁸A. Mankofsky, K. Papadopoulos, and A. T. Drobot, Bull. Am. Phys. Soc. **32**, 1787 (1987); Phys. Rev. Lett. **61**, 94 (1988).
- ⁹K. Kamada, C. Okada, T. Ikehata, H. Ishizuka, and S. Miyoshi, J. Phys. Soc. Jpn. **46**, 1963 (1979).
- ¹⁰F. Wessel and S. Robertson, Phys. Fluids **24**, 739 (1981).
- ¹¹L. Spitzer, *Physics of Fully Ionized Gases* (Wiley, New York, 1962).
- ¹²N. R. Pereira, N. Rostoker, and J. S. Pearlman, J. Appl. Phys. **55**, 704 (1984).
- ¹³F. S. Felber, R. O. Hunter, Jr., N. R. Pereira, and T. Tajima, Appl. Phys. Lett. **41**, 705 (1982).
- ¹⁴T. Tajima, J. Koga, and T. Fujinami, EOS Trans. Am. Geophys. Union **68**, 1400 (1987).
- ¹⁵R. Hong, F. J. Wessel, J. Song, A. Fisher, and N. Rostoker, J. Appl. Phys. **64**, 73 (1988).